Interstitial Equal-Phased Arrays for EM Hyperthermia

PAUL F. TURNER, MEMBER, IEEE

Abstract —Microwave radiating antenna arrays frequently have been inserted directly into cancerous tumors to heat directly and destroy the tumor cells. Example heating patterns are shown with a simple antenna design. An improved design is also described and power absorption patterns are calculated by a three-dimensional numerical model. This model is used to show effects of frequency and applicator design on the power pattern. The numerical model is also applied to show an improved power pattern with a synchronous (equal-phase) compared to a nonsynchronous array. The model shows that an increase in tip capacitance increases the heating at the tip.

I. Introduction

THE EVALUATION OF implanted electromagnetic (EM) antennas into a tumor (to heat it from the inside) has been reported since 1978 [1]–[3]. As the desire to heat invasively larger masses grew, other researchers began to use arrays of applicators which were sequentially connected to an EM generator [4]. In February 1979, BSD Medical Corporation began experimental treatments of swine with synchronous interstitial EM coaxial antennas operated at 600 to 1000 MHz. A patent was filed on the technique on June 19, 1979, and eventually was granted [5]. The first synchronous microwave interstitial system was placed in clinical use in January 1980. The same month the author published the basic technique and principles [6]. In June 1980, Strohbehn reported numerical predictions of various sizes of synchronous interstitial arrays which was later published [7].

The first clinical treatments with the synchronous interstitial arrays began in July 1980 at Loma Linda School of Medicine using the BSD-1000 Hyperthermia System. Although substantial tumor response to the treatment was observed as a result of these early clinical trials, the clinicians were generally not in favor of so much invasion into the tumor site.

In the last two years, the interest in using the interstitial applicator arrays has greatly increased because of increased popularity of interstitial ionizing radiation therapy. This treatment involves radioactive seeds or wires which are inserted into an array of parallel plastic tubes (interstitially placed in the tumor). Once the plastic tubes are in place, the EM applicator arrays can be inserted to heat the tumor before or after the standard radiation treatment. This interstitial radiation allows a higher dose to be delivered directly to the tumor. When combined with interstitial hyperthermia, the "ionizing radiation resistant" cells are expected to be treated effectively by the hyperthermia, thus providing an increase in the number of tumor cells destroyed [8]. The typical clinical application of this combined treatment is initially expected to be in the head, neck, and breast areas, possibly prior to radical surgery. The use of these microwave interstitial arrays was approved by the United States Food and Drug Administration after successful clinical investigations, which employed concurrent external or interstitial ionizing radiation with most of the hyperthermia treatment.

Previous applicator designs have resulted in a cold zone at the tip requiring insertion beyond the tumor. This is particularly undesirable in brain and neck tumors, where major vessels and critical tissues are located.

II. Materials and Methods

The microwave interstitial applicator is basically a monopole radiator. The insulated center conductor of a coaxial transmission line is extended beyond the end of the outer conductor to a length of approximately half the wave length in the tissue media surrounding the applicator, see Fig. 1(a). Also, an improved design developed by the author is shown in which the center and outer conductor diameters are enlarged. The tip of this center conductor is connected to the enlarged collar (as shown in Fig. 1(b)) (patent pending). This design increases the tip heating and reduced the heating near the point of outer and inner conductor separation. This has been observed in many qualitative experiments rapidly heating clear muscle phantom material with an imbedded thermo-sensitive liquid crystal sheet. The simple center conductor of Fig. 1(a) has a reduction of the current in the tip zone (typical of resonant monopoles). This tends to cause a "cold-tip" for heating the surrounding tissue. This trend can be modified by the increase in the center conductor diameter at the tip to substantially increase the coupling capacitance through the dielectric catheter or tube into which the applicator is inserted. The capacitance per meter of length through which the energy must couple to the tissue is: $C = 2\pi\epsilon_0 k/\ln(b/a)$, f/m where "k" is the relative permittivity of the catheter media, "b" is the outer tube diameter, "a" is the metal lead diameter, and ϵ_0 = free-space permittivity. Therefore, the effect on the voltage distribution of the dielectric insulator around the antenna can be accounted for in part by calculating the capacitance distribution. The

Manuscript received December 3, 1985, revised December 30, 1985.
The author is with BSD Medical Corporation, Salt Lake City, UT 84108.
IEEE Log Number 8607619.

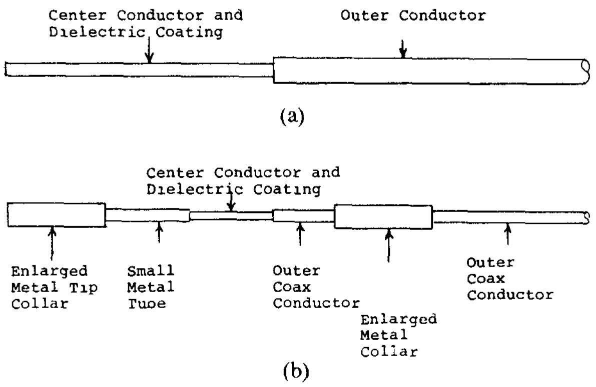

Fig. 1. Coaxial interstitial antenna designs: (a) Center conductor and dielectric extended beyond the outer conductor. (b) Enlarged collar on the tip and outer conductor.

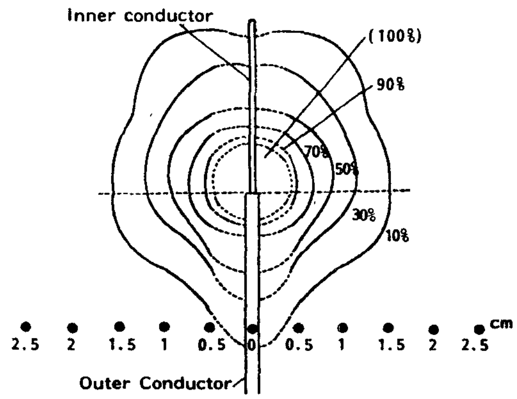

Fig. 2. Relative power absorption pattern measured in muscle phantom at 680 MHz. Measured after 9 W of input power for 5 min. 100 percent is a temperature change of 19.4°C to a level of 42.8°C.

low-dielectric catheter loading causes the antenna voltage and current fields to become like a capacitive quasi-static field passing through the catheter. The increased tip capacitance provides increased tissue loading of the tip. A normal monopole in free space has an open circuit at the tip resulting in the tip current null. The enlarged collars of Fig. 1(b) are each 1.07-mm diameter and 9.5 mm long. The small metal tube is 0.86-mm diameter and 9.5 mm long. The outer coax is 0.95-mm diameter and extends 0.64 mm beyond the outer conductor collar. The exposed dielectric-coated center conductor is 0.2-mm diameter and 9.5 mm long.

Since the dielectric tubing surrounding the applicator has a small value permittivity, the length of the monopole is quite small compared to the wavelength within the tubing. This results in a strong dependence of this coupling capacitance to the distribution of the quasi-static fields into the conductive tissue. The result is that the "cold-tip" characteristic can be substantially overcome by the increase in displacement current flowing from the enlarged tip into the tissue. The increased tip capacitance may also provide a more uniform current phase along the center conductor, because of the circuit series effect which is comprised of the lead inductance and tip capacitance.

Testing of these small applicators is difficult since the power absorption pattern changes rapidly with radial distance from the applicator. One test method used was to rapidly heat gel muscle phantom tissue and monitor temperature change. Accurate measurements are difficult, since the temperature changes caused by the heating can begin to smear over such small distances from the thermal conduction in the tissue. Also, accurate placement of the nonmetallic temperature sensors is difficult in the gel phantom.

Another testing method that can be used is scanning the EM fields with small E-field sensors. This method overcomes the thermal conduction problem, but still causes difficulty in obtaining precise positioning of the sensor. Thus, numerical modeling becomes a desirable method of modeling these applicators due to the limited test capabilities of other methods and potential test design improvements obtained through numerical modeling.

Numerical modeling of interstitial applicators has been reported by other researchers [8]–[10]. Part of the results presented in this manuscript were obtained using a three-dimensional model developed by the author [11]. This method is based on modeling the amplitude and phase of the applicators by an array of point source dipoles. The equations for a point source dipole are well known in the literature, thus they will not be repeated here [11]–[13]. The dominant field in the central heat pattern is the field parallel with the antennas for $\phi = 0$ which is

$$\vec{E}_{1\phi} = \frac{-J_e \mu \cos\phi e^{-\gamma r}}{4\pi j\omega\epsilon^*}\left[\frac{1}{r^3} + \frac{\gamma}{r^2} + \frac{\gamma^2}{r}\right]\hat{\phi}$$

where J_e is the point-source dipole displacement current, r is the radial distance from the point source to the observation point, ω is the radians per second, ϵ^* is the complex permittivity, μ is the permeability, and γ is the medium propagation constant where $\gamma^2 = -\omega^2\mu\epsilon^*$.

The vector summation of these small model sources enables a three-dimensional solution of the field within the space enclosed by the array. The coupling characteristics of the applicator are inputs to the model by specifying the amplitude and phase distribution of the point source elements. Such a model allows various phase and amplitude distributions to be modeled and compared to provide design guidance in optimizing applicator arrays. The model is not an exact solution for a device unless the amplitude and phase distributions are properly specified. The model allows even impractical distributions to be analyzed.

This numerical method was also used to compare the results with that reported by Trembly as a test case [9]. In both the author's method and the Trembly method, the effect of coupling among the applicators was neglected.

III. Results

Fig. 2 is the measured total rise of temperature over 5 min of heating which includes both power absorption and heat conduction effects of the gel phantom. The result of the long 5-min heating time shows little tip heating. The true power absorption curve must be measured with heating times of less than 30 s for such a small heat zone.

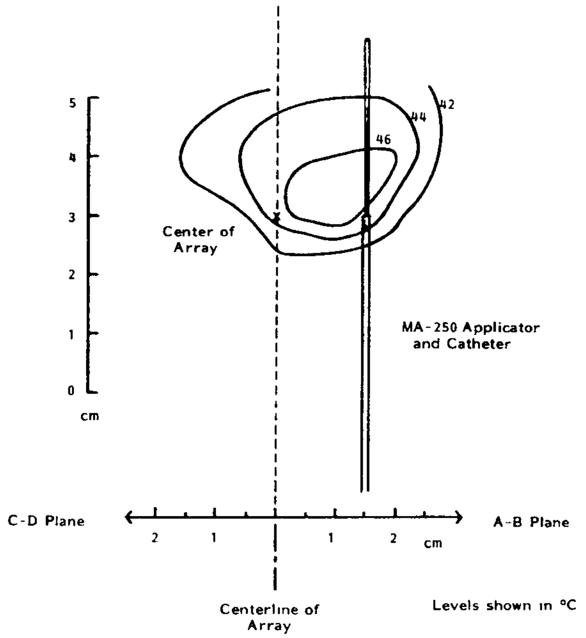

Fig 3 Steady-state temperature distribution in a flank of an anesthetized swine following 20 min of heating with 14 W at 680 MHz. A square array of four applicators with 2-cm spacing was used. Plane AB is shown to the right of center line passing through an applicator. Plane CD is shown to the left passing between applicators.

The pattern of temperature change was measured in the flank muscle tissue of an anesthetized swine for an array of four applicators. The temperature pattern is shown in Fig. 3 for an array spacing of 2.1 cm between applicators inserted in a square pattern. The contours were measured after the temperature had been maintained in the tissue for 20 min with 14 W of power at 680 MHz. The dash line indicates the center of the array. The A-B plane shown to the right is the planar pattern obtained along the plane containing the array center and one of the applicators. The pattern shown on the left is the planar pattern along another plane C-D containing the array center but passing midway between the applicators. The pattern shows substantial heating of the center of the array located near the point of separation of the center conductor from the outer conductor. Less temperature elevation was seen between neighboring applicators in plane C-D than near the applicator shown in plane A-B. Note the patterns of both Figs. 2 and 3 show low heating at the applicator tip. This could make applicators difficult to use in areas such as the brain where insertion beyond the tumor into normal tissues may not be possible. Also, the heating is confined to the region of separation between the center and outer coax conductor, causing a small axial length, a length smaller than many typical tumor sizes. The dielectric coating around the coax center conductor was left in place, and no modifications were made to extend the heating to the tip. It has been observed in other tests that if the applicator was operated inside a dielectric catheter, the pattern would elongate along the outer conductor, thus increasing the axial size. This characteristic is desirable for increased heat pattern size for a larger treatment, but does not eliminate the cold tip characteristic.

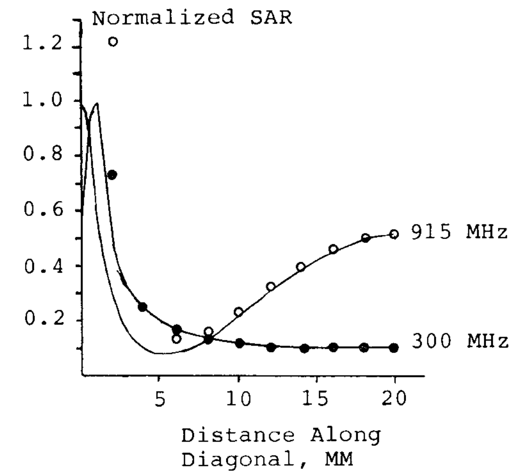

Fig. 4. Comparison of numerical method with previously published data by Trembly (solid curves). Normalized SAR is plotted along a diagonal path in the central heating zone of a square array of four antennas. The media modeled is brain tissue. The data points are predicted by the author's method.

The numerical method developed by the author has been used to model the heating fields of an array of applicators, and comparisons with the calculations of Trembly show good correlation, excluding the area closest to the applicator (less than 4 mm). Trembly assumes a linear phase change within radial distance from the applicator, which is not true for the near field, as more correctly modeled by the author's technique. This may explain some of the variation between these two techniques.

Fig. 4 shows a comparison with the Trembly methods. The comparison was made for an exposed center length of 3 cm and a 2.8-cm applicator spacing along the diagonal axis of the square insertion pattern of the array. The closest correlation appeared to be with the applicator fields assumed as uniform along each element (current distribution) and a uniform radiating phase along the length of the applicator. The data points shown by circles predict higher heating near the applicators than was shown by Trembly (solid curves). The curves beyond 4 mm are in good agreement.

Figs. 5 and 6 are a planar solution of the predicted relative power-absorption patterns at 630 and 915 MHz, respectively, along the diagonal plane for the square insertion pattern of the array. The dielectric characteristics of human muscle were used in the model. The plots are all normalized to 100 percent at 2-mm distance from the applicator's center axis to permit more direct pattern comparison. The model was not used to predict the pattern closer than 2 mm to the antenna, since the number of modeling point dipoles along each antenna was only 80. The element current distribution and phase is assumed to be uniform along the applicator zone; free-space dipoles, of course, would not have a uniform phase and amplitude, but when implanted in a lossy media, the element phase and current distributions will become more uniform. These two patterns are for a 2-cm spacing between the neighboring applicators of the square-matrix insertion pattern. The plots are along the diagonal with a 2.8-cm diagonal sep-

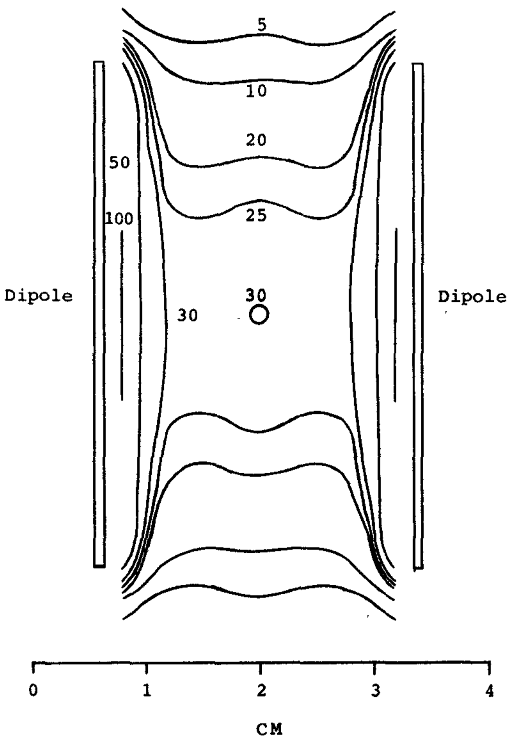

Fig. 5. Planar diagonal pattern of power absorption for a synchronous square array of four antennas: Frequency = 630 MHz, $F(y) = 1$, $k = 52.5$, and $\sigma = 1.5$ mho/m.

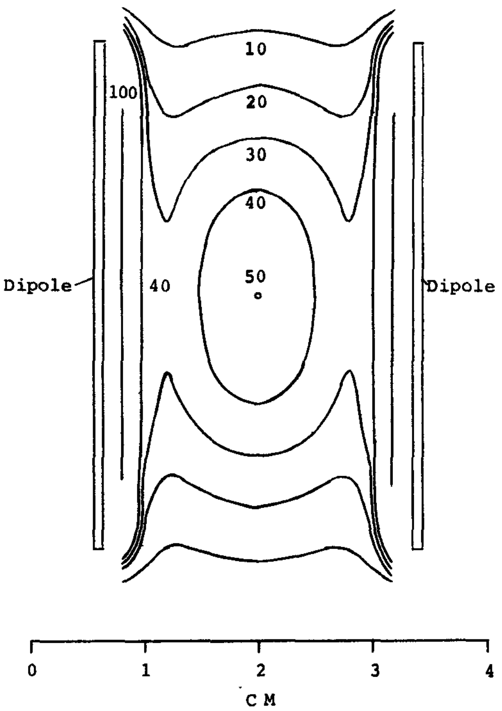

Fig. 6. Planar diagonal pattern as shown in Fig. 5. $F(y) = 1$, frequency = 915 MHz, $k = 51$, and $\sigma = 1.6$ mho/m.

aration distance between opposing applicators as shown (similar to Fig. 4). The voltage amplitude distribution modeled along the antennas $F(y)$ is to be uniform. The phase is also modeled as uniform along the antennas. The muscle dielectric constant (k) and conductivity (σ) are shown. Note that the applicator tip heating appears to be

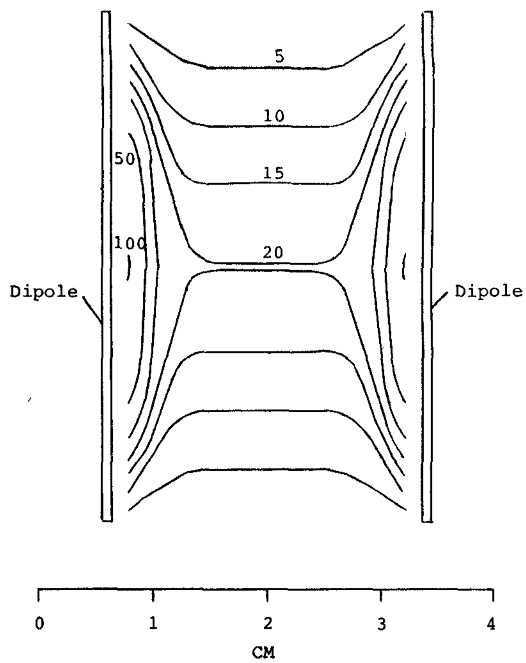

Fig. 7. Planar diagonal pattern as shown in Fig. 5. $F(y) =$ cosine, frequency = 630 MHz, $k = 52.5$, and $\sigma = 1.5$ mho/m.

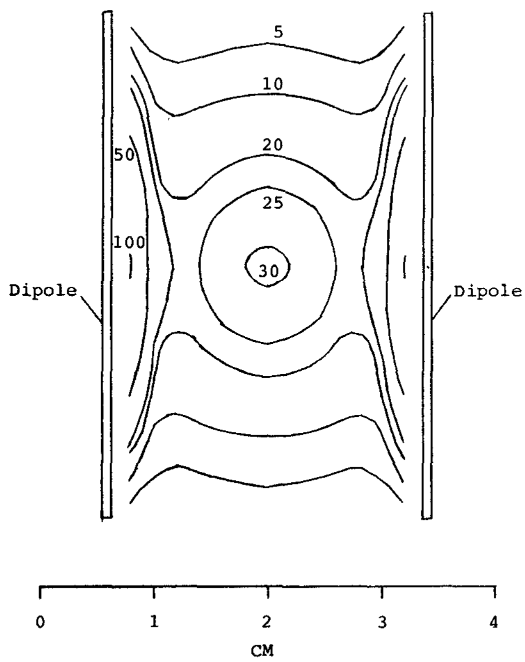

Fig. 8. Planar diagonal pattern as shown in Fig. 6. $F(y) =$ cosine, frequency = 915 MHz, $k = 51$, and $\sigma = 1.6$ mho/m.

greater than that actually obtained in the measurements of Figs. 2 and 3. This suggests that the actual distribution in the applicator type shown in Fig. 1(a) is more like a cosine function typical of monopoles and dipoles.

Figs. 7 and 8 show the same array configuration as Figs. 5 and 6 except the amplitude distribution along the modeled aperture was assumed to be a half-cycle cosine, with central maximum. The cold tip similar to Figs. 2 and 3 is observed in these predictions. The reduction in tip heating is also shown to reduce the uniformity along the central axis of the array (parallel to the applicators).

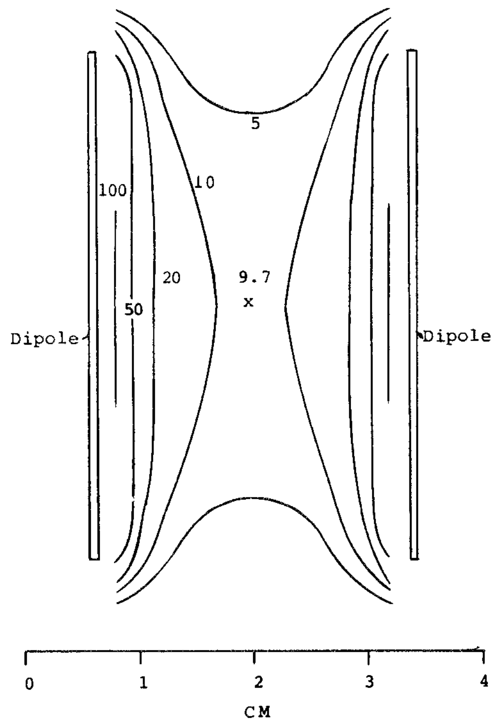

Fig 9. Nonsynchronous array similar to Fig. 5. Planar diagonal pattern for a square array of four antennas: $F(y)=1$, frequency = 915 MHz, $k=51$, and $\sigma=1.6$ mho/m.

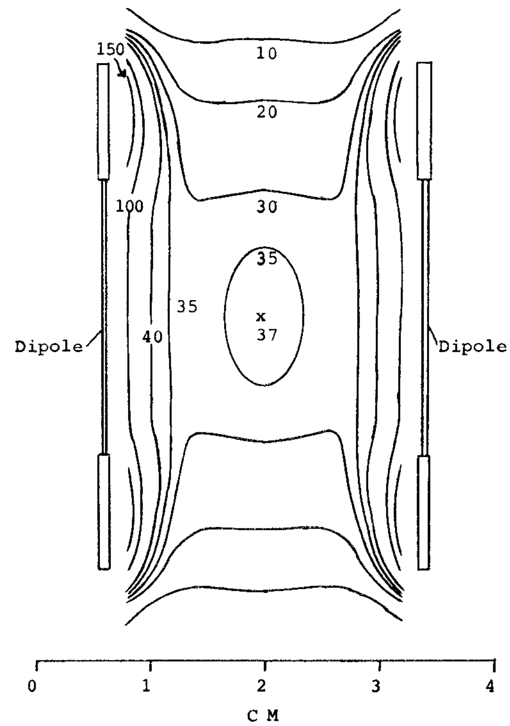

Fig. 10. Planar diagonal pattern as shown in Fig. 5, $F(y)=1$ except $F(y)=1.5$ at the tip collars. Frequency = 630 MHz, $k=52.5$, and $\sigma=1.5$ mho/m.

Prior to our use of synchronous interstitial arrays in 1979, other researchers had been using nonsynchronous arrays by sequentially radiating from applicators arranged in an array. The power absorption pattern for the nonsynchronous array is shown in Fig. 9, with other parameters identical to that of the synchronous array of Figure 6. The 630-MHz pattern was calculated to be identical to Fig. 9. Note the five-fold improvement in central heating by the synchronous array.

The numerical model was then used to model the enlarged diameter tip and outer coax section of Fig. 1(b). This applicator was modeled with a uniform amplitude and phase distribution through the region of smaller diameter and an increase of 1.5 times in current density in the enlarged zones. This model was used because the capacitance of the enlarged zone is about twice that of the intermediate enlarged zone and is much higher than the insulated center conductor zone. The actual distributions are a function of distributed lead capacitance and inductance which is not exactly calculated in the model. However, phantom testing of the applicator described in Fig. 1(b) has shown uniform heating along each enlarged collar which is twice the power absorption along the radiation zone between the two collars. This results in a measured heating pattern length of about 5 cm.

Figs. 10 and 11 show the predicted patterns of power absorption resulting from this estimated applicator illumination. Note that the entire central zone of Fig. 10 is quite uniform, even extending toward the tip region along the central axis. A very local increase in heating is observed near the enlarged collars which is twice that of the zone between the collars. This is the same as the measured distribution. Our experience with animal testing would suggest the increased tip heating zone will have temperatures limited by cooler blood flowing into the periferal zone of the heating pattern. The volume enclosed by this increased heating level at the tip is quite small. The tip heating shown is very desirable for brain and neck areas. The configuration of Fig. 11 was tested in gel muscle phantom. The rate of heating at the tip zone was about double the dipole center and the array central zone. These observations were made with a liquid crystal sheet submerged in clear phantom.

The predicted pattern of Fig. 11 shows more selective central focusing than Fig. 9 but similar heating field enhancement toward the tip of the applicator array. The heating shown by Figs. 10 and 11 is similar to that observed in phantom testing (not shown) with the modified applicator design of Fig. 1(b). The numerical model has also been used to predict the potential effect of varying the phase distribution along the dipole element. Although some of these phase conditions may be difficult to design, some design optimization may be possible through such studies (not included). Further, measurements to refine the match between various applicator distributions and the present design is expected to improve clinical utility of this numerical method. It is useful to observe the type of heat patterns achievable with capacitive tip modification of the amplitude distribution designed to eliminate tip cold spots. The configuration of Fig. 11 was tested with a temperature sensor at the array center and a sensor imbedded within each of the applicators 1.9 cm from the center conductor

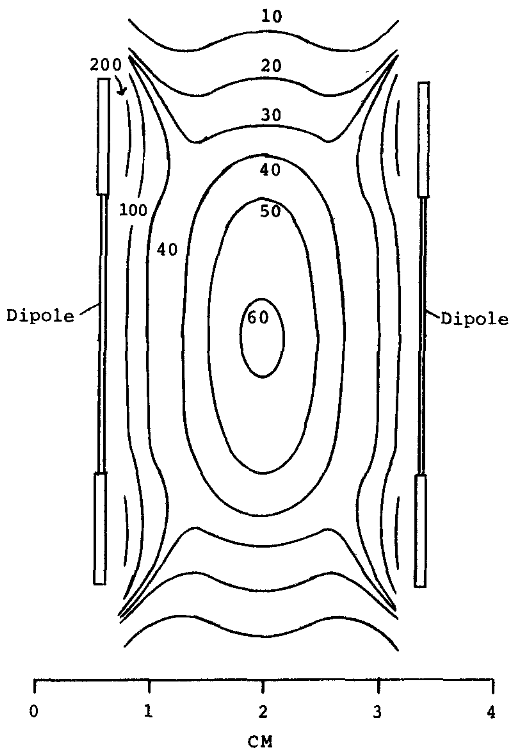

Fig. 11. Planar diagonal pattern as shown in Fig. 6. $F(y)=1$ except $F(y)=1.5$ at the tip collars. Frequency = 915 MHz, $k=51$, and $\sigma=1.6$ mho/m.

tip. A forward power of 20 and 1.7 W reflected was applied to the array. The imbedded sensors of the four applicators detected temperature rise (after 80 s of heating) of 3.4, 3.9, 4.1, and 4.4°C. The corresponding change measured at the array center was 4.1°C. After 7 min of heating the imbedded sensors had detected changes of 9.9, 11.6, 10.5, and 10.9°C with a corresponding 16.1°C change in the array center. At this time, power was turned off and after one min, the temperatures dropped 2.2, 2.7, 2.9, and 2.9°C in the imbedded sensors. The array center cooled 2.2°C. These tests show that the temperature gradients actually obtained may be more uniform than the predicted power absorption.

IV. Summary

The use of the microwave interstitial antenna arrays operated synchronously has been found to provide quite uniform heating fields, which extend to the tip zone of the applicator when enlarged diameter coaxial sections are used. Numerical modeling of applicator arrays provide a useful tool to evaluate design parameter changes to these arrays and applicators, which may enable further improvements in applicator design. The use of arrays of four applicators in a square insertion pattern (each square side being 2 cm) appears to provide heating power uniformly distributed to a substantial degree within much of the volume enclosed by the array. The use of synchronous (equal-phase) interstitial arrays improves the heating to the central region of the array as compared to nonsynchronous arrays. The further extension of the numerical model to various amplitude and phase distributions should lead to further applicator design improvements.

References

[1] L. Taylor, "Electromagnetic syringe," *IEEE. Trans. Biomed. Eng.*, vol. BME-25, no. 3, pp. 303–304, May 1978.

[2] L. Taylor, "Brain cancer therapy using an implanted microwave radiator," *Microwave J.*, pp. 66–71, Jan. 1981.

[3] L. Taylor, "Implantable radiators for cancer therapy by microwave hyperthermia," *Proc. IEEE*, vol. 68, no. 1, pp. 142–149, Jan. 1980.

[4] J. Strohbehn *et al.*, "Localized hyperthermia in dog brain using an invasive microwave probe," presented at Int. IEEE/APS Symp. Nat. Radio Sci. Meeting, Seattle, WA, June 19, 1979.

[5] P. Turner, "Invasive hyperthermia apparatus and method," U.S. Patent No. 4448198, May 15, 1984.

[6] J. Short and P. Turner, "Physical hyperthermia and cancer therapy," *Proc. IEEE*, vol. 68, no. 1, pp. 133–142, Jan. 1980.

[7] W. Dewey, "Interaction of heat with radiation and chemotherapy," Cancer Res. Suppl. 55, no. 10 CNREA, pp. 4714S–4720S, Oct. 1984.

[8] J. Strohbehn *et al.*, "Evaluation of an invasive microwave antenna system for heating deep-seated tumors," NCI Monograph 61, NIH Publ. No. 82-2437, pp. 489–491, June 1982.

[9] B. Trembly, "The effects of driving frequency and antenna length on power deposition within a microwave antenna array used for hyperthermia," *IEEE Trans. Biomed. Eng.*, vol. BME-32, no. 2, pp. 152–157, Feb. 1985.

[10] R. King, *et al.*, "The electromagnetic field of an insulated antenna in a conducting or dielectric medium," *IEEE Trans. Microwave Theory Tech.*, vol. MTT-31, pp. 574–583, July 1983.

[11] P. Turner and L. Kumar, "Computer solution for applicator heating patterns," NCI Monograph No. 61, NIH Publ. No. 82–2437, pp. 521–523, June 1982.

[12] R. Harrington, *Time-Harmonic Electromagnetic Fields*. New York: McGraw–Hill Book Co., 1961, p. 79.
[13] W. Weeks, *Electromagnetic Theory for Engineering Applications*. New York: John Wiley and Sons, Inc., 1964, p. 310.

Paul F. Turner (S'70–M'79) was born in Salt Lake City, UT, on April 19, 1947. He received the B.S.E.E. degree in 1971 and the M.S.E.E. degree in 1983, both from the University of Utah.

He initially specialized in microwave communications and antenna design for defense systems. In August of 1978, he changed employment to BSD Medical Corporation. Since that time he has been devoted full time to the development and design of microwave and RF applicators and methods for the purpose of hyperthermia cancer treatment. He has obtained nine patents, and several patents are pending related to his work.